Nanoscale

Accepted Manuscript

This article can be cited before page numbers have been issued, to do this please use: L. liu, Q. zhang, S. Tao, C. Z. Zhao, E. Almuti, Q. Al-Galiby, S. Bailey, I. M. Grace, C. Lambert, J. Du and L. Yang, *Nanoscale*, 2016, DOI: 10.1039/C6NR03807G.

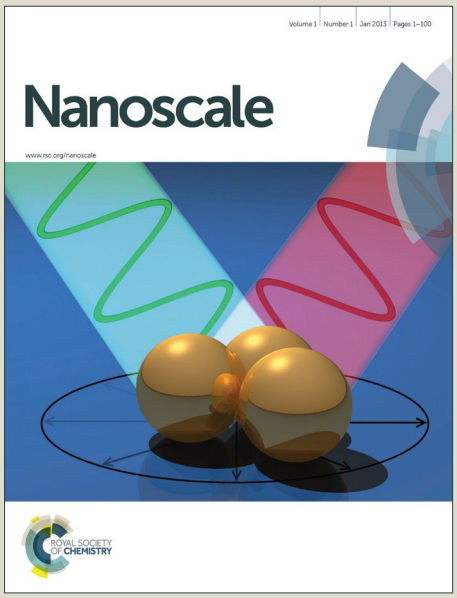

This is an *Accepted Manuscript*, which has been through the Royal Society of Chemistry peer review process and has been accepted for publication.

Accepted Manuscripts are published online shortly after acceptance, before technical editing, formatting and proof reading. Using this free service, authors can make their results available to the community, in citable form, before we publish the edited article. We will replace this *Accepted Manuscript* with the edited and formatted *Advance Article* as soon as it is available.

You can find more information about *Accepted Manuscripts* in the Information for Authors.

Please note that technical editing may introduce minor changes to the text and/or graphics, which may alter content. The journal's standard Terms & Conditions and the Ethical guidelines still apply. In no event shall the Royal Society of Chemistry be held responsible for any errors or omissions in this *Accepted Manuscript* or any consequences arising from the use of any information it contains.

ROYAL SOCIETY OF CHEMISTRY

www.rsc.org/nanoscale

View Article Online
DOI: 10.1039/C6NR03807G

Journal Name

ARTICLE

Received 00th January 20xx,
Accepted 00th January 20xx

DOI: 10.1039/x0xx00000x

www.rsc.org/

Charge transport through dicarboxylic-acid-terminated alkanes bound to graphene-gold nanogap electrodes

Longlong Liu,[a, b] Qian Zhang,[a] Shuhui Tao,[a] Cezhou Zhao,[c] Eman Almutib,[d, e] Qusiy Al-Galiby,[d, e] Steven W. D. Bailey,[d] Iain Grace,[d] Colin J. Lambert,[d] Jun Du[b,*] and Li Yang[a,*]

Graphene-based electrodes are attractive for single-molecule electronics due to their high stability and conductivity and reduced screening compared with metals. In this paper, we use the STM-based matrix isolation I(s) method to measure the performance of graphene in single-molecule junctions with one graphene electrode and one gold electrode. By measuring the length dependence of the electrical conductance of dicarboxylic-acid-terminated alkanes, we find that transport is consistent with phase-coherent tunneling, but with an attenuations factor β_N = 0.69 per methyl unit, which is lower than the value measured for Au-molecule-Au junctions. Comparison with density-functional-theory calculations of electron transport through graphene-molecule-Au junctions and Au-molecule-Au junctions reveals that this difference is due to the difference in Fermi energies of the two types of junction, relative to the frontier orbitals of the molecules. For most molecules, their electrical conductance in graphene-molecule-Au junctions is higher than that in Au-molecule-Au junctions, which suggests that graphene offers superior electrode performance, when utilizing carboxylic acid anchor groups.

Introduction

Measurement of the electrical properties of single molecules located within nano-gap junctions is possible using mechanically-controllable break junctions (MCBJ),[1] scanning-tunneling-microscopy break junction (STM-BJ),[2] I(s) method based on scanning tunneling microscopy (STM),[3] and conductive probe atomic force microscopy (CP-AFM).[4, 5] These methods have been used to create single-molecule junctions exhibiting a range of functionalities, including rectifiers,[6, 7] field effect transistors[8] and molecular switches.[9] To date most single-molecule electronical measurements have focused on the use of gold contacts, due to their chemical stability, lack of oxidation, high conductivity and ease of junction fabrication. However, gold has a number of drawbacks, including its non-compatibility with complementary metal-oxide-semiconductor (CMOS) technology and high atomic mobility. For this reason, other metals such as Pt, Ag, Pd[10] have been explored for their potential to form electrodes in single-molecule junctions and a range of anchor groups such as amine,[11] pyridine,[4] carboxylic acids[2, 12–14] and thiol have been assessed for their ability to make electrical contact to such electrodes. However, all of the above single-molecule metallic junctions exhibit large fluctuations

[a] Department of Chemistry, Xi'an-Jiaotong Liverpool University, Suzhou, Jiangsu 215123, China. Email: li.yang@xjtlu.edu.cn
[b] Department of Chemistry and Chemical Engineering, Chongqing University, Chongqing 400044, China. Email: dujune@cqu.edu.cn
[c] Department of Electrical Electronic Engineering, Xi'an-Jiaotong Liverpool University, Suzhou, Jiangsu 215123, China.
[d] Department of Physics, Lancaster University, Lancaster LA1 4YB, UK.
[e] Department of Physics, Al-Qadisiyah University, Al-Qadisiyah, Iraq.

Electronic Supplementary Information (ESI) available on details of the theoretical conductances of graphene-molecule-Au junctions. See DOI: 10.1039/x0xx00000x

View Article Online
DOI: 10.1039/C6NR03807G

and instabilities and therefore in the search for more controllable contacts, nonmetallic electrodes are now being considered.[15]

Recently, carbon-based materials have been used as nonmetallic electrodes for the investigation of molecular junctions.[16] González et al.[17] performed the theoretical study of carbon-based STM tips and explained the advantages of using those novel tips compared with standard metallic tips. Yan et al.[15] fabricated carbon/molecule/carbon junctions by electron beam evaporation, with molecular layers covalently bonded to a carbon substrate. These junctions were formed with a high yield and exhibited excellent reproducibility with greater stability and lower tendency for electron migration compared to similar structures using metal contacts. Liu et al.[18] successfully coated Au AFM tips with more than 4-layer graphene using chemical vapor deposition (CVD). The graphene tip shows very small tip-to-tip variation, excellent operational stability, good endurance, and long shelf-life in the formation of molecular junctions. Likewise, Guo et al.[19] revealed a way to harness the diversity and functionality inherent to molecules in electrical devices by covalently bridging gaps in single-walled carbon nanotubes. Marquardt et al.[20] formed a rigid solid-state device with the core of a rod-like molecule between two metallic single-walled carbon nanotube electrodes and observed electroluminescence. Kim et al.[21] designed a series of graphite/amine-terminated oligophenyl/Au molecular hybrid junctions with the STM-BJ technique and measured the conductance of the junctions. Rectification was observed and explained further by calculations which opens up the possibility of assembling molecular junctions with dissimilar electrodes. More recently electroburnt graphene junctions are being developed for contacting single molecule,[22-28] and form a new class of electrodes, which may be advantageous also in allowing reduction of the effects of defects in the electrodes[29] through the use of extended planar anchor groups.[30, 31]

These fundamental studies, combined with the availability of relatively defect-free wafer scale graphene[32, 33] suggest that carbon-based materials have the potential to be valuable alternative electrode materials for molecular electronics in the next generation of nanostructured devices.. As a first step towards realizing this potential, we demonstrate the use of graphene as bottom electrode in place of the more-commonly used gold. We measure the conductance of various lengths of bicarboxylic alkanes in Au|dicarboxylic acid|graphene junctions using the STM-based matrix isolation I(s) method in which the STM tip is brought close to the graphene surface without making contact. The formation of the carboxylic acid group with gold is achievable through electronic coupling between the carboxylate group and the gold surface. For each molecule, the conductance histograms reveal well-defined peaks, and in some cases multiple sets of conductance values. The statistically-most-probable conductance values are sensitive to the alkane length and decrease exponentially with increasing molecular length.

Results and discussions

Figure 1(a) shows the STM image of a representative graphene area and reveals that the graphene substrate has the multilayer structure with the defects probably introduced during the CVD process.

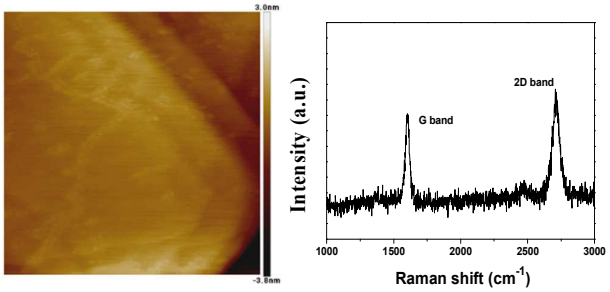

Figure 1. (a) STM image of graphene substrate at 100 nm field of view. (b) Raman spectrum of graphene substrate on nickel with the laser excitation at 532 nm.

Figure 1(b) presents the representative Raman spectrum with two sharp peaks approximately at 1600 and 2700 cm^{-1} distinctly, which can be ascribed to the characteristic peaks of graphene G band and 2D band.The intensity of 2D peak is slightly larger than the G peak. Raman spectra have used to estimate the number of graphene layers in thin flakes on a SiO_2 surface.[34, 35] This approach suggests that the graphene substrate is mainly monolayer or bilayer graphene and therefore of sufficient quality for forming single-molecule junctions.

Figure 2a shows four typical I(s) curves exhibiting current plateaus. The smallest current plateau appears at 1.56 nA, and other current plateaus were found to be a multiple of the smallest fundamental unite (1.56 nA). After dividing by the applied bias, the corresponding conductance curves were generated. The representative conductance histogram for succinic acid constructed from approximately 400 individual current traces was obtained as show in Figure 2b. A clear peak at 15.6 nS (with 4.3 half of the full width half maximum) observed in the conductance histogram can be ascribed to the single molecule conductance of succinic acid in the system and also another peak obviously was about two times of the

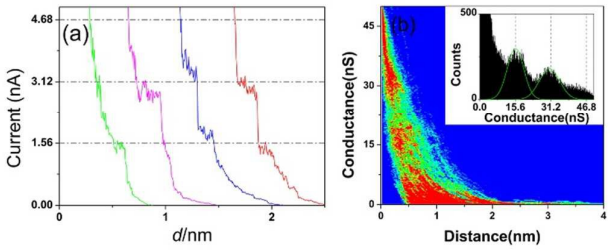

Figure 2. (a) Typical I-s curves collected by the I(s) method under 100 mV. (b)The two-dimensional (2D) histograms of single molecule conductance of the Au-HOOC-$(CH_2)_2$-COOH-graphene constructed from 400 curves. Inset is the corresponding conductance histogram.

View Article Online
DOI: 10.1039/C6NR03807G

single molecule conductance. According to previous work,[13] the single-molecule conductance of succinic acid in the junction formed with gold electrodes is $2.7\times10^{-4}G_0$ = 20.9 nS (where $G_0=2e^2/h \approx$ 77.4 μS, G_0 is the conductance quantum), which is only a little bigger than that of ours. Zhou et al.[36, 37] used electrochemistry scanning tunneling break junction (EC-STMBJ) methods to measure the conductance of succinic acid junctions with different metal (Pb, Ag, Cu) electrodes. The corresponding conductance was 9 nS, 16.5 nS and 18.2 nS for Pb, Ag, Cu electrodes, respectively. Our succinic acid junction with graphene and gold electrodes has a conductance value similar to that observed using Ag and Cu electrodes, bigger than that obtained using Pb electrodes and smaller than the conductance value for succinic acid binding to Pd (23 nS) under electrochemistry conditions.[38] These differences highlight the fact that the conductance of metal–molecule–metal junctions depends on the energies of the frontier molecular orbitals relative to the Fermi levels of the electrode,[39] details of the electrode conformation in the vicinity of the anchor groups, molecular conformation,[40, 41] the nature of the surrounding medium and junction asymmetry.[42, 43].

In order to understand the mechanism of charge transport in the molecule and to investigate the length dependence of conductance, we measured the conductance of HOOC-$(CH_2)_n$-COOH (n=3~6) molecules in contact gold and graphene electrodes. The same parameters were used in all measurements, except when measuring the rather small conductance of octanedioic acid, the bias voltage was increased to 500 mV to minimise the impact due to the instrumental errors.

Figure 3 presents the conductance histograms of the alkanedicarboxylic acids, from which the most probable conductances are found to be 10.3±2.8, 5.1±1.2, 2.4±0.5 and 1.08±0.34 nS for pentanedioic acid (a), hexanedioic acid (b), heptanedioic acid (c), octanedioic acid (d), respectively. Here, the conductance is more likely a representative value mixed by various types of conductance in different geometries junctions. This is due to short testing current window and relatively weak contact compared to other symmetric metal molecular junctions. It is clear that the conductance values decrease with increasing molecular length. Just
as for butanedicarboxylic acid, in some cases we observe pronounced peaks located at integer multiples of the single-molecule-conductances in accordance with Refs.[2, 12] To compare with literature results using other electrode materials and asymmetric contacts, the conductance of alkanedicarboxylic acids in different molecular junctions were summarized in Table 1. As expected for phase-coherent tunneling,[39] the conductance decreases exponentially with increasing molecular chain length and can be described as Equation (1), where G is the single molecular conductance, A is a constant influenced by the coupling between the contact of molecule and electrode, β_N is the tunneling decay constant that reflects the efficiency of electron transport, N is the number of methylene units. Values for β_N are also presented in Table 1.

$$G = \mathbf{A}\exp(-\boldsymbol{\beta}_N N) \qquad (1)$$

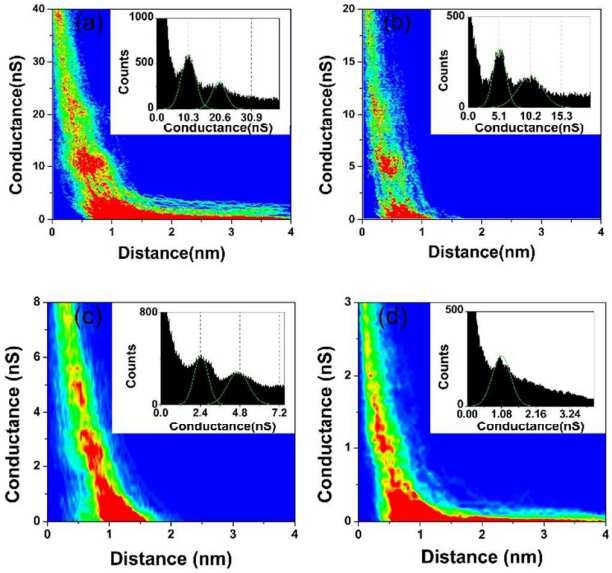

Figure 3. The 2D histograms of single molecule conductance of the Au-HOOC-$(CH_2)_n$-COOH-graphene with (a) n=3, (b) n=4, (c) n=5 and (d) n=6. Insets are the corresponding conductance histograms. All the histograms were constructed from more than 400 curves.

Table 1. Comparison of the conductance of dicarboxylic acid in different junctions.

Molecular junctions	Conductance(nS，HC)					Tunneling decay constant (β_N)
	n=2	n=3	n=4	n=5	n=6	
Au- HOOC-(CH_2)n-COOH-Graphene	15.6	10.3	5.1	2.4	1.08	0.69±0.04
Au- HOOC-(CH_2)n-COOH-Au[14]	20.9	----	3.87	----	0.77	0.81±0.01
Ag- HOOC-(CH_2)n-COOH-Ag[37]	13.2	8	3.7	1.7	----	0.71±0.03
Cu- HOOC-(CH_2)n-COOH-Cu[37]	18.2	7.5	2.9	1.2	----	0.95±0.02
Au-molecule-Au[12]	----	----	----	----	----	0.78
Theory: perfect graphene Au- HOOC-(CH_2)n-COOH-Graphene	38.5	13	5.3	4	2.2	0.69
Theory: defective graphene Au- HOOC-(CH_2)n-COOH-Graphene	27.1	5.19	2.96	1.09	0.68	0.89

Note:"----"represents that the data is unavailable or unadopted from the references.

View Article Online
DOI: 10.1039/C6NR03807G

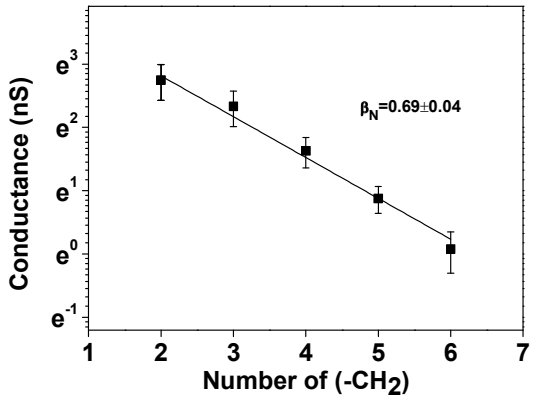

Figure 4. Natural logarithm plots of single molecule conductance versus number of (-CH_2) units for molecular junctions in the Au-HOOC-$(CH_2)_n$-COOH-graphene junction.

Figure 4 shows the relationship between natural logarithm plots of single-molecule conductance and the number of (-CH_2) units in the Au-HOOC-$(CH_2)_n$-COOH-graphene junction. The measured conductance decreases with the molecular length and the linear fit yields a tunneling decay constant of ~0.69 per (-CH_2) unit, which as shown in Table 1 is slightly smaller than that obtaining using Au, Cu and Ag electrodes. Furthermore the conductances of the n=3, 4, 5 and 6 molecules were a slightly bigger than those obtaining using Au, Cu and Ag electrodes, while our value for single-molecule conductance of succinic acid is slightly smaller.

Theoretical calculations

To calculate electrical properties of the molecules in Figure 5 of lengths (n=2, 4 and 6) the relaxed geometry of each isolated molecule was found using the density functional theory (DFT) code SIESTA,[44] which employs Troullier-Martins pseudopotentials to represent the potentials of the atomic cores and a local atomic-orbital basis set. We used a double-zeta polarized basis set for all atoms and the local density functional approximation (LDA-CA) by Ceperley and Adler.[45] The Hamiltonian and overlap matrices are calculated on a real-space grid defined by a plane-wave cutoff of 150 Ry. Each molecule was relaxed to the optimum geometry until the forces on the atoms are smaller than 0.02 eV/Å and in case of the isolated molecules, a sufficiently-large unit cell was used to avoid spurious steric effects.

After obtaining the relaxed geometry of an isolated molecule, the molecule was then placed between graphene and (111) gold electrodes and the molecules plus electrodes allowed to further relax to yield the optimized structures shown in Figures 5a-c (Relaxed structures between two gold electrodes are shown in Figure S2 of the SI.). For each structure in Figures 5a-c and in Figures S2a-c of the SI, we use the Gollum method[46] to compute the transmission coefficient $T(E)$ for electrons of energy E passing from the lower electrode to the upper gold electrode. Once the $T(E)$ is computed, we

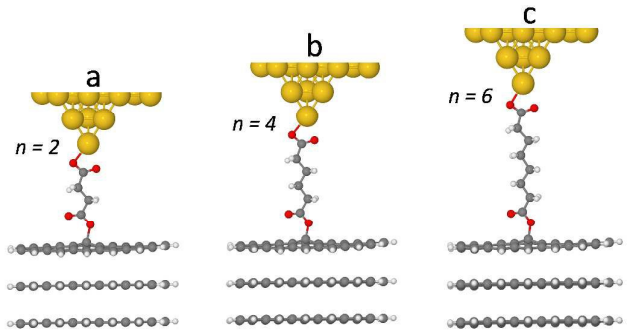

Figure 5. a, b and c show the optimized geometries of systems containing the dicarboxylic-acid-terminated alkane molecule at lengths (n=2, 4 and 6) connected to the graphene-gold electrodes.

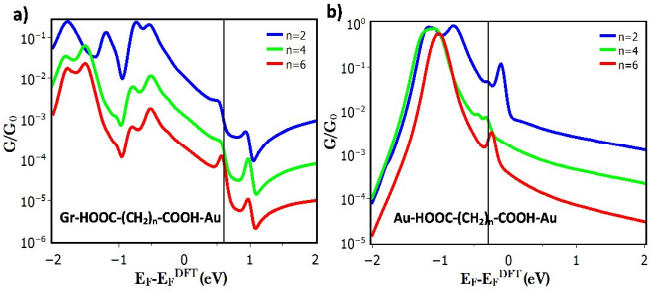

Figure 6. The room-temperature electrical conductance over a range of Fermi energies of the systems containing: a) the dicarboxylic-acid terminated alkane molecule with the length n=2, n=4 and n=6 of CH_2 attached to the graphene-gold electrodes, b) the molecule with the same lengths attached to two gold electrodes.

calculated the zero-bias electrical conductance G using the Landauer formula:

$$G = I/V = G_0 \int_{-\infty}^{\infty} dE T(E) \left(-\frac{df(E)}{dE}\right) \qquad (2)$$

where $G_0 = \left(\frac{2e^2}{h}\right)$ is the quantum of conductance, $f(E)$ is Fermi distribution function defined as $f(E) = \left[e^{(E-E_F)k_BT} + 1\right]^{-1}$ where k_B is Boltzmann constant and T is the temperature. Since the quantity $-\frac{df(E)}{dE}$ is a normalised probability distribution of width approximately equal to k_BT, centred on the Fermi energy E_F, the above integral represents a thermal average of the transmission function $T(E)$ over an energy window of the width k_BT (= 25 meV at room temperature).[39]

For the structures in the Figures 5a-c, Figure 6a shows the room-temperature electrical conductance over a range of Fermi energies E_F. in the vicinity of the DFT-predicted Fermi energy E_F^{DFT}. For a wide range of values of E_F, the conductance decreases with molecular length, in agreement with our experimental measurements. Similarly

View Article Online
DOI: 10.1039/C6NR03807G

Figure 6b shows that for the Au-molecule-Au structures in the Figures S2a-c of the SI, their room-temperature electrical conductances decrease with length. The predicted value of the attenuation coefficient β_N depends on the precise value of E_F and therefore we *computed β_N for a range of Fermi energies. For Au-molecule-Au junctions, the closest fit with experiment was found for* E_F =-0.3 eV relative to E_F^{DFT}, whereas for graphene-molecule-Au junctions, the closest fit was found for E_F - E_F^{DFT} =0.65 eV.

Figure 7 shows a logarithmic plot of predicted single-molecule conductances versus the number of (-CH_2) units in the alkane chain, along with a comparison with experiment. The close agreement between theory and experiment for β_N suggests that the difference between the attenuation coefficients of graphene-molecule-Au and Au-molecule-Au junctions arises from a difference in the positions of their frontier orbitals relative to E_F. Figure 7 also shows that the theoretical conductance values are slightly higher than measured ones for all molecular lengths, which can be attributed to the tendency of LDA to underestimate the HOMO-LUMO gap, which results in an overestimated of the conductance.[47] To examine the role of defects in the graphene substrate, we computed electrical conductances when the lower oxygen of the anchor group binds to a defective site formed by removing a carbon from the graphene sheet and passivating the dangling bonds with hydrogen as show in Figure

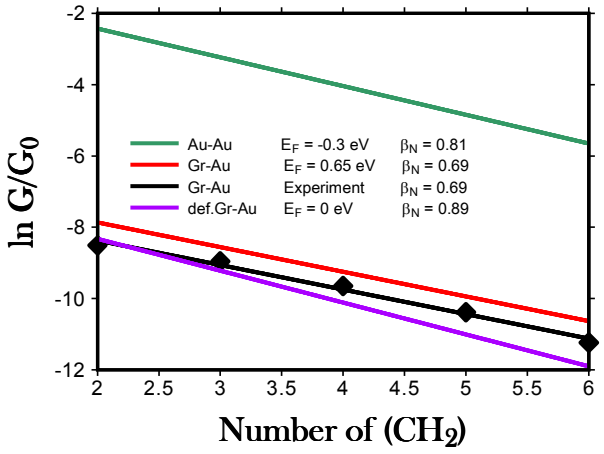

Figure 7. Comparison between theory and experiment of the logarithm of single molecule conductance versus number of (-CH_2) units in dicarboxylic-acid-terminated alkanes. The green, red and purple lines represent the theoretical results obtained using two gold electrodes (green curve) and perfect graphene-gold electrodes (red curve) and defected graphene-gold electrodes (purple curve), respectively. The black line shows the experimental measurements. The values of the Fermi energy E_F (relative to E_F^{DFT}) giving the closest fit to experiment depends on the nature of the contact. For Au-Au, the best fit is found at E_F= -0.3 eV and yields a decay constant of β_N = 0.81. For Gr-Au, the closest fit is found at E_F = 0.65 eV and yields β_N = 0.69. For defect graphene contact (def. Gr-Au) we found E_F= 0.0 eV, β_N = 0.89. These compare with the experimental decay constant of β_N = 0.69.

S5. The resulting conductances are shown in the bottom row of Table 1 and a comparison with experiment shown in Figure 7. These show that defects lower the conductance and increase the attenuation coefficient and that the measured results lie between the defective of defect-free theoretical values.

Experimental

The gold substrates (10 mm×10 mm) were purchased from Arrandee made in Germany and the Au (111) surfaces annealed under a butane flame in a dark room. The gold substrate was placed into the flame until it glowed dark red and then cooled to room temperature for 30 seconds. This flame annealing process was repeated three times to obtain Au (111) terraces. The surface structure was examined by Bruker STM instrument (Multimode 8, USA). Graphene on nickel substrates prepared by CVD were purchased from Graphene-supermarket (USA). The graphene was characterized by Raman spectroscopy on XploRATM plus (Horiba, USA) with the laser excitation at 532 nm. Scans were taken over an extended range (1000 ~ 3000 cm^{-1}) and the exposure time was 30 s. 99.99% Gold wire of 0.25 mm diameter was purchased from Tianjing Lucheng Metal and the gold STM tips were prepared using electrochemical etching method reported by Ren in 2004.[48] The etching solution consisted of hydrochloric acid and ethanol with 1:1 volume ratio. A gold wire with 0.25 mm diameter was curved into a ring with a diameter of about 6-8 mm, then the gold ring was horizontally placed on the surface of the solution with about 3/4 height of the ring immersed in the solution. Another 0.25 mm diameter gold wire was immersed in the centre of the gold ring vertically. The immersed length is normally about 1-2 mm. 4 V was selected as the etching voltage in our study after a careful investigation of tip morphology under scanning electron microscope (SEM). The gold substrate or the graphene substrate was immersed into a freshly prepared ethanol solution containing 3 mM alkanedicarboxylic acids for 5 min to form a self-assembled monolayer (SAM), followed by washing in 2 mL ethanol and then drying with an Ar flow. The conductance of each molecule was measured on the Multimode 8 STM under room temperature in air using the I(s) method, which measures the conductance of single molecule junctions formed by repeating moving the tip extremely close to the substrate surface but without contacting and then withdrawing from the surface. During this process, the terminal anchor groups of the molecule could attach to both the STM tip and the substrate and form a molecular junction. Thousands of traces of current versus distance (I-s) were then recorded for statistical analysis. All the experiments were performed at a bias voltage of 100 mV unless otherwise stated.

Conclusions

In conclusion, we have demonstrated that graphene is a viable electrode material for single-molecule electronics and for molecules terminated by carboxylic-acid anchor groups mainly leads to an increase in the electrical conductance compared with Au-molecule-Au junctions. By measuring their length dependence, we find that transport is consistent with phase-coherent tunneling, but with an attenuation factor β_N = 0.69 per methyl unit, which is lower than

View Article Online
DOI: 10.1039/C6NR03807G

the value measured for Au-molecule-Au junctions. Comparison with density-functional-theory calculations of electron transport through graphene-molecule-Au junctions and Au-molecule-Au junctions reveals that this difference is due to the difference in Fermi energies of the two types of junctions, relative to the frontier orbitals of the molecules.

Conflict of interest

The authors declare no competing financial interest.

Acknowledgements

The authors would like to thank Richard. J. Nichols for helpful comments concerning the conductance measurement. This work was supported by the National Natural Science Foundation of China (NSFC Grants 21503169), the Jiangsu Science and Technology programme (BK 20140405), Suzhou Industrial Park Initiative Platform Development for Suzhou Municipal Key Lab for New Energy (RR0140), the XJTLU Research Development Fund (PGRS-13-01-03), EPSRC project UK EPSRC (Grant nos. EP/M014452/1 and EP/N017188/1), by the EU ITN MOLESCO project number 606728, The Ministry of Higher Education and Scientific Research, Al Qadisiyah University, IRAQ and the Ministry of Education, Taif University, Saudi Arabia.

Notes and references

1 J. Moreland, J. W. Ekin, J. Appl. Phys. 1985, 58, 3888.
2 B. Q. Xu, N. J. Tao, Science 2003, 301, 1221.
3 W. Haiss, H. van Zalinge, S. J. Higgins, D. Bethel, H. Höbenreich, D. J. Schiffrin, R. J. Nichols, J. Am. Chem. Soc. 2003, 125, 15294.
4 B. Q. Xu, X.Y. Xiao, N. J. Tao, J. Am. Chem. Soc. 2003, 125, 16164.
5 X. D. Cui, A. Primak, X. Zarate, J. Tomfohr, O. F. Sankey, A. L. Moore, T. A. Moore, D. Gust, G. Harris, S. M. Lindsay, Science 2001, 294, 571.
6 A. S. Martin, J. R. Sambles, G. J. Ashwell, Phys. Rev. Lett. 1993, 70, 218.
7 M. L. Chabinyc, X. X. Chen, R. E. Holmlin, H. Jacobs, H. Skulason, C. D. Frisbie, V. Mujica, M. A. Ratner, M. A. Rampi, G. M. Whitesides, J. Am. Chem. Soc. 2002, 124, 11730.
8 N. J. Tao, Phys. Rev. Lett. 1996, 76, 4066.
9 J. Chen, M. A. Reed, A. M. Rawlett, J. M. Tour, Science 1999, 286, 1550.
10 V. M. García-Suárez, A. R. Rocha, S. W. Bailey, C. J. Lambert, S. Sanvito, J. Ferrer, Phys. Rev. B, 2005, 72, 045437.
11 D. V. Leff, L. Brandt, J. R. Heath, Langmuir 1996, 12, 4723.
12 S. Martín, W. Haiss, S. Higgins, P. Cea, M. C. López, R. J. Nichols, J. Phys. Chem. C 2008, 112, 3941.
13 Y. H. Wang, Z. W. Hong, Y. Y. Sun, D. F. Li, D. Han, J. F. Zheng, Z. J. Niu, X. S. Zhou, J. Phys. Chem. C 2014, 118, 18756.
14 F. Chen, X. L. Li, J. Hihath, Z. F. Huang, N. J. Tao, J. A. Chem. Soc. 2006, 128, 15874.
15 H. J. Yan, A. J. Bergren, R. L. McCreery, J. Am. Chem. Soc. 2011, 133, 19168.
16 Y. J. Dappe, C. González, J. C. Cuevas, Nanoscale 2014, 6, 6953.
17 C. González, E. Abad, Y. J. Dappe, J. C. Cuevas, Nanotechnology 2016, 27, 105201.
18 Y. G. Wen, J. Y. Chen, Y. L. Guo, B. Wu, G. Yu, Y. Q. Liu, Adv. Mater. 2012, 24, 3482.
19 X. F. Guo, J. P. Small, J. E. Klare, Y. L. Wang, M. S. Purewal, Iris W. Tam, B. H. Hong, R. Caldwell, L. M. Huang, S. O'Brien, J. M. Yan, R. Breslow, S. J. Wind, J. Hone, P. Kim, C. Nuckolls, Science 2006, 311, 356.
20 C. W. Marquardt, S. Grunder, A. B aszczyk, S. Dehm, F. Hennrich, H. V. Löhneysen, M. Mayor, R. Krupke, Nat. Nanotechnol. 2010, 5, 863.
21 Taekyeong Kim, Zhen-Fei Liu, Chulho Leed, Jeffrey B. Neaton, Latha Venkataramana, PNAS 2014, 111, 10928.
22 X. F. Song, J. L. Hu, H. B. Zeng, J. Mater. Chem. C 2013, 1, 2952.
23 E. Burzurí, F. Prins, H. S. J. van der Zant, Graphene 2012, 1, 26.
24 A. Barreiro, F. Börrnert, M. H. Rümmeli, B. Büchner, L. M. K. Vandersypen, Nano Lett. 2012, 12, 1873.
25 Y. Lu, C. A. Merchant, M. Drndic, A. T. C. Johnson, Nano Lett. 2011, 11, 5184.
26 H. Sadeghi, J. A. Mol, C. S. Lau, G. A. D. Briggs, J. Warner, C. J. Lambert, PNAS 2015, 9, 2658.
27 H. Sadeghi, S. Sangtarash, C. L. Lambert, Physica E: Low-dimensional Systems and Nanostructures 2015 http://dx.doi.org/10.1016/j.physe.2015.09.005i
28 H. Sadeghi, S. Sangtarash, C. J. Lambert, Beilstein journal of nanotechnology 2015, 6, 1413.
29 C. J. Lambert, D. L. Weaire, Metallography 1981, 14, 307.
30 S. Bailey, D. Visontai, C. J. Lambert, M. R. Bryce, H. Frampton, D. Chappell, J. Chem. Phys. 2014, 140, 054708.
31 C. G. Péterfalvi, C. J. Lambert, Phys. Rev. B 2012, 86, 085443.
32 E. Lörtscher, Nat. Nanotechnol. 2013, 8, 381.
33 Y. Cao, S. H. Dong, S. Liu, Z. F. Liu, X. F. Guo, Angew. Chem. 2013, 52, 3906.
34 A. C. Ferrari, J. C. Meyer, V. Scardaci, C. Casiraghi, M. Lazzeri, F. Mauri, S. Piscanec, D. Jiang, K. S. Novoselov, S. Roth, A. K. Geim, Phys. Rev. Lett. 2006, 97, 187401.
35 M. Velický, D. F. Bralley, A. J. Cooper, E. W. Hill, I. A. Kinloch, A. Mishchenko,K. S. Novoselov, H. V. Patten, P. S. Toth, A. T. Valota, S. D. Worrall, R. A. W. Dryfe, ACS Nano 2014, 8, 10089.
36 Z. L. Peng, Z. B. Chen, X. Y. Zhou, Y. Y. Sun, J. H. Liang, Z. J. Niu, X. S. Zhou, B. W. Wei, J. Phys. Chem. C 2012, 116, 21699.
37 Y. H. Wang, X. Y. Zhou, X. Y. Sun, Y. Y. Sun, D. Han, J. F. Zheng, Z. J. Niu, X. S. Zhou, Electrochemical Acta 2014, 123, 205.
38 L. Mühlbacher, J. Ankerhold, C. Escher, J. Chem. Phys. 2004, 121, 12696.
39 C. J. Lambert, Chem. Soc. Rev. 2015, 44, 875.
40 C. M. Finch, S. Sirichantaropass, S. W. Bailey, I. M. Grace, V. M. García-Suárez, C. J. Lambert, J. Phys.: Condens. Matter, 2007, 20, 022203.
41 M. Berritta, D. Z. Manrique, C. J. Lambert, Nanoscale 2015, 7, 1096.
42 J. G. Kushmerick, C. M. Whitaker, S. K. Pollack, T. L. Schull, R. Shashidhar, Nanotechnology 2004, 15, S489.
43 S. Martín, D. Z. Manrique, V. M. García-Suarez, W. Haiss, S. J. Higgins, C. J. Lambert, R. J. Nichols, Nanotechnology 2009, 20, 125203.
44 J. M. Soler, E. Artacho, J. D. Gale, A. García, J. Junquera, P. Ordejón, D. Sánchez-Portal, J. Phys.: Condens. Matter 2002, 14, 2745.
45 D. M. Ceperley, B. J. Alder, Phys. Rev. Lett. 1980, 45, 566.
46 J. Ferrer, C. J. Lambert, V. M. García-Suárez, D. Z. Manrique, D. Visontai, L. Oroszlany, R. Rodríguez-Ferradás, I. Grace, S. Bailey, K. Gillemot, H. Sadeghi, L. A. Algharagholy, New J. Phys. 2014, 16, 093029.

View Article Online
DOI: 10.1039/C6NR03807G

47 a) S. Y. Quek, M. Kamenetska, M. L. Steigerwald, H. J. Choi, S. G. Louie, M. S. Hybertsen, J. B. Neaton, L. Venkataraman, Nat. Nanotechnol. 2009, 4, 230; b) W. J. Hong, D. Z. Manrique, P. Moreno-García, M. Gulcur, A. Mishchenko, C. J. Lambert, M. R. Bryce, T. Wandlowski. J. Am. Chem. Soc. 2012, 134, 2292; c) Y. H. Li, B. Masoud, Al ‐ Galiby Qusiy, D. Z. Manrique, G. X. Zhang, J. Hamill, Y. C. Fu, P. Broekmann, W. J. Hong, T. Wandlowski, D. Q. Zhang, C. J. Lambert, Angew. Chem. Int. Ed. 2015, 54, 13586.
48 B. Ren, G. Picardi, B. Pettinger, Rev. Sci. Instrum. 2004, 75, 837.